9-1-1999

Experimental Optimization of Confined Air Jet Impingement on a Pin Fin Heat Sink

L. A. Brignoni

S V. Garimella
Purdue Univ, sureshg@purdue.edu

Experimental Optimization of Confined Air Jet Impingement on a Pin Fin Heat Sink

Luis A. Brignoni and Suresh V. Garimella

***Abstract*— A variety of nozzle configurations were tested to characterize and optimize the performance of confined impinging air jets used in conjunction with a pin-fin heat sink. Four single nozzles of different diameters and two multiple-nozzle arrays were studied at a fixed nozzle-to-target spacing, for different turbulent Reynolds numbers ($5000 \leq \mathrm{Re} \leq 20\,000$). Variations in the output power level of the heat source and nozzle-to-target spacing were found to have only modest effects on heat transfer at a fixed Reynolds number. Enhancement factors were computed for the heat sink relative to a bare surface, and were in the range of 2.8–9.7, with the largest value being obtained for the largest single nozzle (12.7 mm diameter). Average heat transfer coefficients and thermal resistance values are reported for the heat sink as a function of Reynolds number, air flow rate, pumping power, and pressure drop, to aid in optimizing the jet impingement configuration for given design constraints.**

***Index Terms*— Air jets, confined jets, electronics cooling, heat sinks, heat transfer, jet impingement, pin fins.**

NOMENCLATURE

A_h	Exposed area of heat source, m^2.
C	Clearance between nozzle plate and fin tip, m.
c_p	Specific heat, J/kg · K.
d	Orifice diameter, m.
H	Nozzle-to-target spacing $(L + C)$, m.
$\overline{h}$	Average heat transfer coefficient, W/m^2· K.
k	Thermal conductivity, W/m · K.
L	Heat sink height, m.
l	Orifice length (nozzle plate thickness), m.
n	Number of nozzles in a given array.
Pr	Fluid Prandtl number ($\mu \cdot c_p$/k).
Q_{gen}	Power supplied to heater, W.
Q_{loss}	Power losses, W.
Q_{out}	Convected heat, W.
Re	Reynolds number $[4\rho(\dot{\mathrm{V}}/n)/\pi$ d $\mu]$.
R_{conv}	Convective thermal resistance, °C/W.
R_{int}	Interface thermal resistance, °C/W.
S	Interjet spacing (multiple nozzles), m.
T_{jet}	Jet exit temperature, °C.
T_{base}	Heat sink base temperature, °C.
T_s	Heat source surface temperature, °C.
T_∞	Ambient temperature, °C.
U_{jet}	Mean jet velocity, m/s.
$\dot{\mathrm{V}}$	Volume flow rate, ft^3/min (cm^3/s).

Greek:

ε	Enhancement factor $(\overline{h}_{\mathrm{enhanced}}/\overline{h}_{\mathrm{bare}})$.
Φ	Pumping power, W.
ΔP	Pressure drop, Pa.
μ	Viscosity, kg/s · m.
ρ	Mass density, kg/m^3.

Manuscript received October 22, 1998; revised April 6, 1999. This paper was recommended for publication by Associate Editor T.-Y. T. Lee upon evaluation of the reviewers' comments. This work was supported in part by Cray Research, Chippewa Falls, WI, and an Advanced Opportunity Program Fellowship, University of Wisconsin, Milwaukee.

L. A. Brignoni is with the Department of Mechanical Engineering, University of Wisconsin, Milwaukee, WI 53201 USA.

S. V. Garimella is with the School of Mechanical Engineering, Purdue University, West Lafayette, IN 47907-1288 USA (e-mail: sureshg@ecn.purdue.edu).

Publisher Item Identifier S 1521-3331(99)07016-6.

I. INTRODUCTION

JET IMPINGEMENT has been widely used in many applications where high convective heat transfer rates are required. In confined jet impingement the spent fluid from a single nozzle or an array of nozzles flows outward in a narrow channel bounded by the plate containing the nozzle and the impingement surface. The heat transfer in such an impingement arrangement, especially with surface enhancement present, needs to be better understood in order to optimize the performance of this cooling technique.

The literature on jet impingement is extensive and detailed reviews are available (e.g., [1]). A majority of these studies have involved liquid and air jet impingement on smooth (unenhanced) surfaces. Garimella and Rice [2] characterized confined and submerged single impinging jets of FC-77 (a perfluorinated, dielectric liquid) in terms of the effects on local heat transfer of nozzle geometry (d and l/d), nozzle-to-target spacing H/d, and flow rate. Schroeder and Garimella [3], [4] conducted a similar study with air jets using single and multiple orifices. Obot and Trabold [5] studied the consequences of blocking the spent air, which resulted in cross flow in the confinement region. Heat removal rates have been found to be markedly enhanced by increasing the number of orifices at fixed Reynolds numbers, especially at small H/d [4], [5].

Studies of jet impingement used in conjunction with extended surfaces have reported promising results. Sullivan *et al.* [6] reported enhancements of as much as 80% for experiments using roughened spreader plates with liquid (FC-77) jet impingement. Hansen and Webb [7] evaluated the heat transfer enhancement for six fin geometries and two nozzle diameters. They reported heat transfer enhancements ranging from 1.5 to 4.5 using single jets of air. Variation of nozzle-to-target spacing H/d was found to have little effect on heat transfer in the range of $1 \leq H/d \leq 5$. Copeland [8] reported heat transfer coefficients as high as

38 500 W/m^2 · K with multiple slot jets in impingement and suction using FC-72 and pin-fin arrays. With multiple round nozzles, Copeland [9] obtained even higher heat transfer coefficients, with enhancement factors of up to 4.5 relative to smooth-surface experiments.

Heat transfer with extended surfaces has also been studied in cross flow across pin-fin heat sinks. Minakami *et al.* [10] used a wind tunnel facility to study experimental optimization of fin spacing in pin-fin heat sinks. They found that small increments in air velocity caused large increases in heat transfer coefficients for a given heat sink. Chapman *et al.* [11] tested an elliptical pin-fin heat sink to describe its thermal performance; significant heat fluxes (6.2 W/cm^2) were obtained at relatively low cross flow air velocities ($\leq$ 4 m/s). Lee *et al.* [12] used a porous metal foam heat sink to remove 100 W from a 1 cm^2 chip in a personal computer application.

The present study seeks to understand the effects of the governing variables in confined air jet impingement on enhanced surfaces including nozzle diameter, flow rate, nozzle-to-target spacing and number of nozzles, in an effort to optimize the impingement configuration for a given pin-fin heat sink. Pressure-drop measurements were also obtained in order to optimize thermal performance with respect to pumping power. A single, highly effective copper pin-fin heat sink was chosen for this study; jet parameters were varied while the heat sink remained the same for all experiments.

II. Experimental Setup and Procedures

The experiments were conducted in the same facility as used in a previous study on confined air jet impingement on bare (unenhanced) surfaces [3], [4]. A schematic of the air jet impingement facility used for the experiments is shown in Fig. 1. A regenerative blower with a variable-speed drive is the prime mover. The air flow is measured by one of three flowmeters mounted in parallel, depending on the range. Several valves in conjunction with the variable-speed drive controller help to set the required flow rate. The air is then delivered to a flow-conditioning cylindrical plenum in the test section. Interchangeable nozzle plates are attached to the lower end of the plenum; the nozzle plate serves to confine the flow to being radially outward after impingement. The nozzle-to-target spacing H is set using three high-precision gage blocks. Complete details of the test section are presented in Schroeder [13]. The static pressure in the plenum is measured using a pressure tap located in the wall connected to a manometer. The temperature of the air jet is measured using a 36 gauge T-type thermocouple located just prior to the plenum exit. Four different orifice diameters were studied for the single-nozzle experiments: $d = 1.59$, 3.18, 6.35, and 12.7 mm; two configurations were studied for multiple-nozzle experiments: an array of four 3.18 mm diameter nozzles (4 $\times$ 3.18), and another with nine 1.59 mm diameter nozzles (9 $\times$ 1.59). The spacing between multiple nozzles was fixed at $S/d = 4$. All orifices have an aspect ratio l/d of 1 (the nozzle plate thickness was fabricated to be equal to the nozzle diameter for each plate).

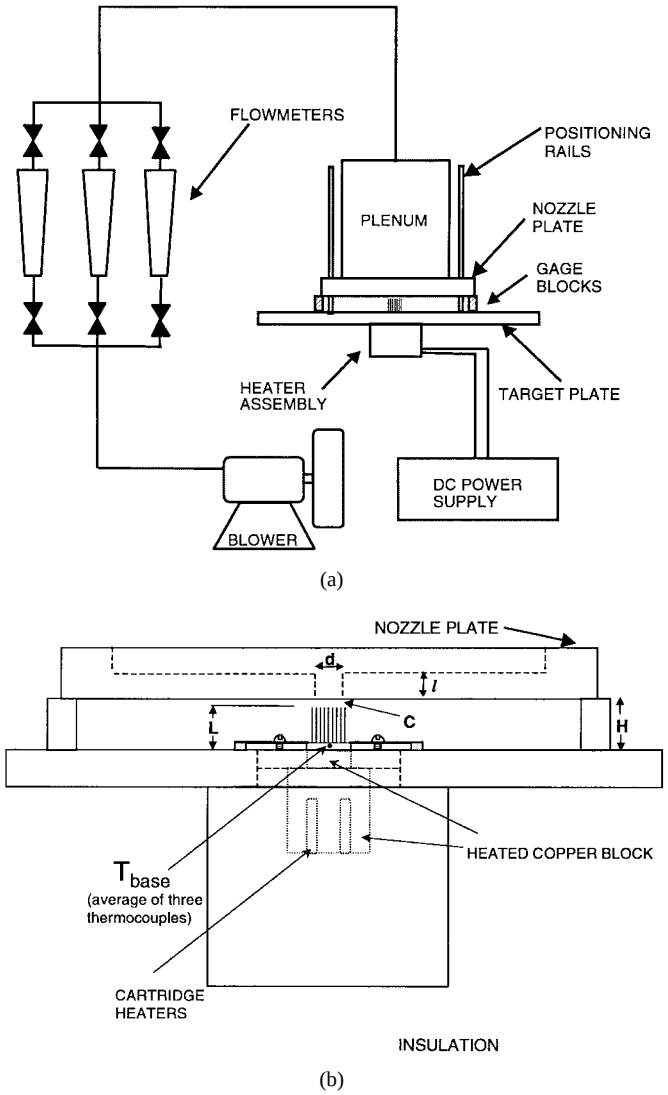

Fig. 1. (a) Schematic diagram of the air jet impingement facility. (b) Heater assembly and nomenclature used for geometric parameters. Three gage blocks are used in a triangular pattern to set H, and are small enough to cause negligible obstruction to the radial outflow.

The primary goal of Schroeder and Garimella [3], [4] was to obtain *local* heat transfer coefficients on the surface, and hence, an electrically heated stainless steel foil heater was used in their study. For the present study the focus is on *average* heat transfer coefficients and hence an isothermal copper block heater was designed [see Figs. 1(b) and 2]. Three 100-W cartridge heaters were imbedded into the heated block, which was made from 99.99% pure oxygen-free copper. Five holes of 1 mm diameter were drilled from the bottom of the block to insert 36 gauge T-type thermocouples which measure the surface temperature distribution in the simulated chip as shown in the figure. The variation in readings from the five thermocouples was never greater than 0.5 °C. A simulated chip of square cross section was machined at the top of the round copper rod. A 20 $\times$ 20 mm square heated surface, flush-mounted to the target plate, is thus exposed to the jet [Figs. 1(b) and 2]. The copper block was well insulated to ensure that a major portion of heat generated was lost to convection through the exposed top surface. The voltage drop

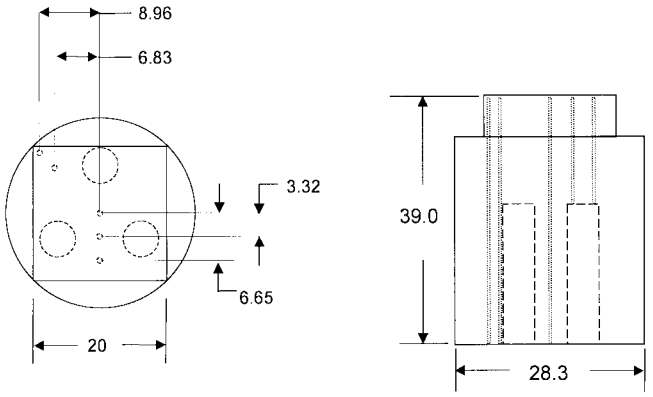

(a) (b)

Fig. 2. Details of cartridge-heater and thermocouple locations in the heated copper block (all dimensions are in mm).

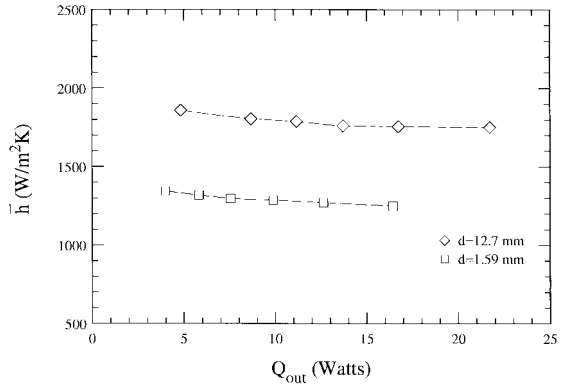

Fig. 3. Variation of heat sink average heat transfer coefficient with different values of convected heat, at Re = 10 000.

across the cartridge heaters was measured; the current was determined from the voltage drop across a calibrated resistance shunt mounted in series with the circuit. The heat generation is determined as a product of the measured voltage and current.

The losses by conduction through the insulation and by free convection from the exposed top surface of the heater assembly were determined experimentally in a manner similar to that of Obot and Trabold [5]. In the absence of flow, and at steady state, an electrical power input is required to obtain a temperature difference $(T_s - T_\infty)$. A linear relationship was experimentally found between this power generated (Q_{loss}) and the surface-to-ambient temperature difference

$$Q_{\text{loss}} = 0.096 \cdot (T_s - T_\infty). \tag{1}$$

The losses (Q_{loss}) ranged from 8–26% of the power input (Q_{gen}) for the enhanced-surface experiments; $T_\infty \equiv T_{\text{jet}}$ when impingement air flow is turned on. For each experiment, attainment of steady state was carefully verified by ensuring that temperature measurements were invariant over successive 15-min intervals. The average heat transfer coefficient in the impingement heat transfer experiments, for the unenhanced (bare surface) and enhanced cases, is obtained by

$$\overline{h}_{\text{bare}} = \frac{Q_{\text{out}}}{A_h \cdot (T_s - T_{\text{jet}})} \tag{2a}$$

$$\overline{h}_{\text{enhanced}} = \frac{Q_{\text{out}}}{A_h \cdot (T_{\text{base}} - T_{\text{jet}})} \tag{2b}$$

in which Q_{out} is the difference between Q_{gen} and Q_{loss}. The heat sink base temperature T_{base} is determined as the average of the readings from three thermocouples inserted into the base of the heat sink and spaced equally along its diagonal. In both equations, the heat transfer coefficient is based on the bare surface area, A_h, of 20 mm $\times$ 20 mm, which is identical to the heat sink base area.

The heat sink (PinFin, Inc.) is held on to the heat source by cantilever clamps, which exert a repeatable, constant force. The heat sink has a 20 by 20 mm copper base, which is 2.4 mm thick. The copper pin fins are of circular cross section with a 0.9 mm diameter, and are 16.4 mm high. The heat sink has a total of 72 pins with a pin-to-pin spacing of 1.59 mm. The interface material clamped between the heat sink and the heated surface is T-pli 210 (Thermagon, Inc.); the measured thermal resistance of this material was nominally 0.2 °C/W. The uncertainty in measured heat transfer coefficients at 95% confidence was estimated to range from 5.5–14.2% for bare-surface experiments, and from 2.9–5.8% in the presence of the heat sink. The greatest contribution (73%) to the estimated uncertainties in the heat transfer coefficient resulted from uncertainties in the temperature measurement. The maximum uncertainty of 14.2% corresponds to the experiment with the bare surface at Re $=$ 5000 for a single 12.7 mm diameter nozzle; under these conditions, $\overline{h} = 151$ W/m$^2 \cdot$ K. As a check, this value differs by only 8% from that found from averaging the local heat transfer measurements of Schroeder and Garimella [3], whose uncertainty in $\overline{h}$ was less than 4.5%. The focus of this work is not on bare surface experiments, but instead, on optimizing air jet impingement on a pin-fin heat sink; the uncertainty in $\overline{h}_{\text{enhanced}}$ was never greater than 5.8%.

III. Results

Experiments were performed for Reynolds numbers ranging from 5000 to 20 000 with the nozzle-to-target plate spacing fixed at $H = 21.8$ mm. However, the effects on the results of varying this spacing (and hence, tip clearance) as well as the power output were first studied with the heat sink clamped on to the heat source. Bare and enhanced surface results are then compared at different flow rates and an enhancement factor ε reported for all cases. Some design considerations are explored subsequently.

The effect of varying the amount of convected heat Q_{out} on the average heat transfer coefficient $\overline{h}$ is shown in Fig. 3 for the smallest and largest nozzle diameters used. The figure shows $\overline{h}$ as a function of Q_{out} for Re $=$ 10 000 with the heat sink attached. For the 12.7 mm nozzle, increasing Q_{out} by a factor of 4.5 causes a reduction in $\overline{h}$ of 5.7%. Similarly, for the 1.59 mm nozzle, increasing Q_{out} by a factor of 4.1 reduces $\overline{h}$ by 7%. As expected in forced convection situations, the heat transfer coefficient is thus not a strong function of the heat output.

The effect of changing the nozzle-to-target spacing H, and thus, the tip clearance above the heat sink C $[=H - L$, see Fig. 1(b)], is shown in Fig. 4 for single and multiple nozzles at a fixed Reynolds number of 10 000. Four different values

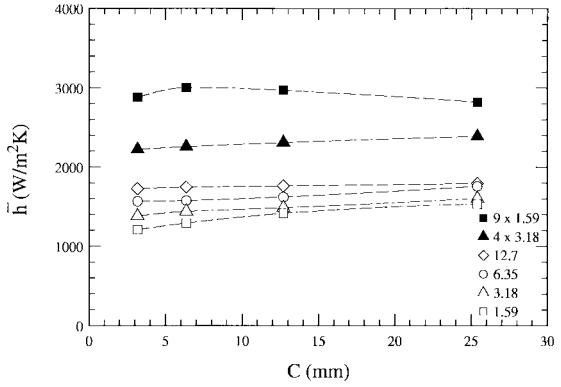

Fig. 4. Effect of nozzle plate-to-fin tip clearance on heat sink average heat transfer coefficient for single and multiple nozzles at Re = 10 000.

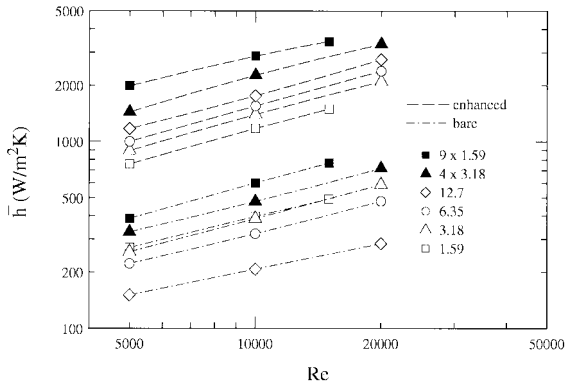

Fig. 5. Comparison between bare and enhanced-surface heat transfer coefficients as a function of Reynolds number for all nozzle configurations tested.

of clearance were studied in these tests: $C = 3.18$, 6.35, 12.7, and 25.4 mm. This parameter is of practical significance since space constraints would dictate that the cooling solution be within the allowable spatial limits without the thermal performance being compromised. In most cases increasing C resulted in a slight increase in $\overline{h}$, as seen in Fig. 4. A possible explanation for this is that for small nozzle diameters and small values of C, the jet impinges deep into the pin-fin array, bypassing the upper portion of the peripheral fins and leaving them almost ineffective. As C is increased the jet flow is rendered radial over a larger span and all of the pin-fins may be used more effectively. Increasing C beyond a certain value, however, does not further enhance heat transfer, and in some cases actually causes a drop in thermal performance, as can be seen in the figure for the 9×1.59 mm array. At large C values the jet may not penetrate the pin-fin array effectively but instead may bypass the pins with the flow being deflected into the clearance area.

It is also observed from Fig. 4 that for the larger nozzle diameters, the variations of $\overline{h}$ with C are modest. For $d =$ 12.7 mm an increase in C from 3.18 to 25.4 mm results in a 3.8% increase in $\overline{h}$. In contrast, for the smallest nozzle diameter ($d = 1.59$ mm), $\overline{h}$ increases by 21% for the same change in C. The results of Hansen and Webb [7] reveal that the heat transfer coefficient for air jet impingement on a pinned surface decreases only slightly as C is increased in the range of spacings $1 \leq H/d \leq 5$, but drops more sharply for $H/d >$ 7. They attributed this reduction in $\overline{h}$ to a reduction in arrival velocity of the fluid as H/d was increased. The present results agree with [7] since the clearances tested here correspond to $1.7 \leq H/d \leq 3.5$ for the $d = 12.7$ mm nozzle, but for the $d = 1.59$ mm nozzle, this range is $13.7 \leq H/d \leq 27.7$.

A fixed clearance of $C = 3.18$ mm was selected for all remaining tests in this study.

Fig. 5 shows $\overline{h}$ as a function of Reynolds number for the bare surface and with the heat sink present. Due to limitations in the pressure drop capabilities of the blower used, the maximum Reynolds number tested for $d = 1.59$ mm and for the 9×1.59 mm array was 15 000. The enhancement factor is defined as $\varepsilon = \overline{h}_{\text{enhanced}}/\overline{h}_{\text{bare}}$ where bare and enhanced heat transfer coefficients are defined in (2). It is emphasized that in the definition of (2b) the resistance introduced by the interface material is excluded from the definition of $\overline{h}_{\text{enhanced}}$ so that $\overline{h}_{\text{bare}}$ and $\overline{h}_{\text{enhanced}}$ may be compared on the same basis. The temperature difference between the heated element surface T_s and the heat sink base T_{base} allowed a determination of experimental values for the interface resistance R_{int}, which was typically ≈0.2 °C/W. However, R_{int} plays no role in the definition of the enhancement factor.

Amongst all the bare-surface experiments it was found that the greatest value for $\overline{h}$ was 767 W/m^2 · K for the 9×1.59 mm nozzle array at Re = 15 000. A value of $\overline{h} = 3437$ W/m^2 · K was obtained with the same nozzle plate at the same Re when the heat sink was attached to the heated surface. This represents an enhancement factor ε of 4.5. The enhancement factors for all the tests were in the range $2.8 \leq \varepsilon \leq 9.7$. The highest value for ε was obtained with the 12.7 mm single nozzle at Re = 20 000.

It is also seen from Fig. 5 that, as expected, the multiple-nozzle arrays yield higher heat transfer coefficients for a fixed Reynolds number, both for the bare surface and with the heat sink present. The heat transfer enhancement resulting from increasing the number of nozzles is stronger with the heat sink clamped on to the heated surface. For $d = 1.59$ mm, when the number of nozzles is increased from 1 to 9, there is a 50% increase in $\overline{h}$ for the bare surface, and a 145% increase for the heat sink, for a given Reynolds number. With $d = 3.18$ mm, these factors are 27 and 62%, respectively, when the number of nozzles is increased from 1 to 4. It must be remembered that these increases (at fixed Re) in heat transfer with the multiple nozzles are obtained at the expense of flow rates of air that are nine or four times higher than the single-nozzle counterparts; however, the pressure drop required is the same for the single and multiple nozzles.

It is interesting to note that for the bare surface, the smaller-diameter nozzles produce the higher heat transfer coefficients, whereas with the heat sink present, the trend is reversed, and the largest nozzle diameter ($d = 12.7$ mm) yields the highest $\overline{h}$.

A. Design Considerations

The foregoing discussion was presented in terms of heat transfer coefficients and Reynolds numbers. However, prac-

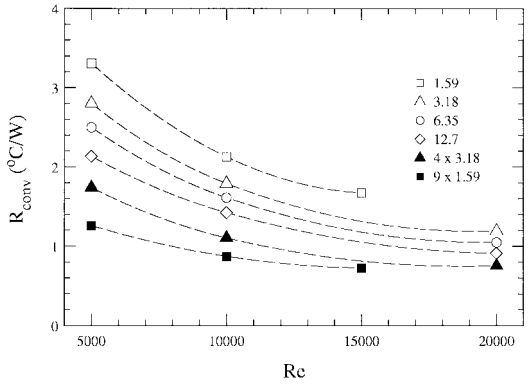

Fig. 6. Heat sink thermal resistance as a function of Reynolds number.

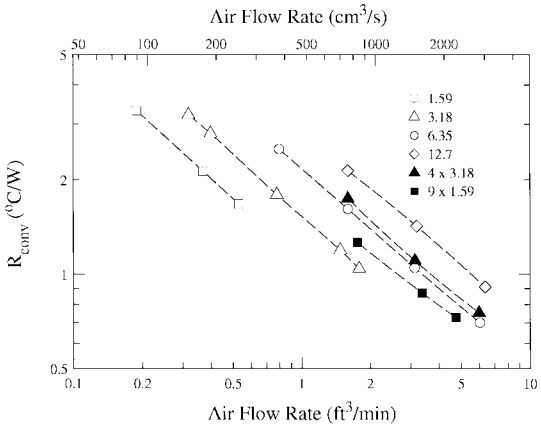

Fig. 7. Heat sink thermal resistance for all nozzle plates at different volumetric air flow rates.

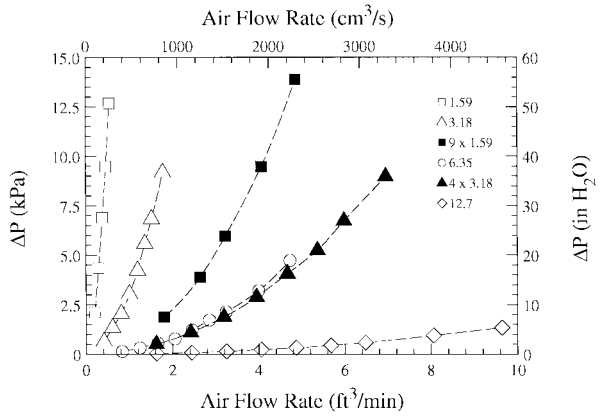

Fig. 8. Pressure drop across the orifices as a function of air flow rate for all nozzle configurations.

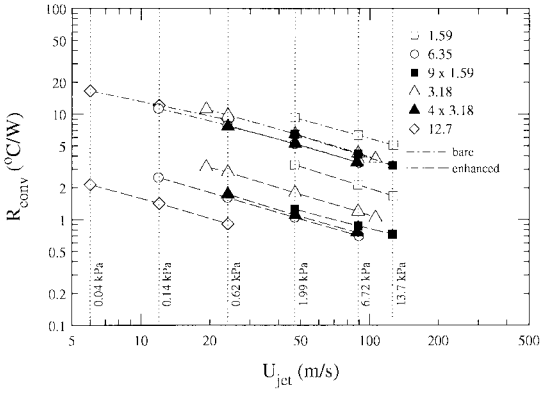

Fig. 9. Thermal resistance of the heat sink and bare surface as a function of mean jet velocity (pressure drop).

tical design choices are usually made based on thermal resistance, air flow rate, pressure drop, and pumping power. In the rest of this paper, results are discussed in terms of these typical design constraints.

In the present study, the thermal resistance R_{conv} of the heat sink is defined as

$$R_{conv} = \frac{T_{\text{base}} - T_{\text{jet}}}{Q_{\text{out}}} \left[\frac{^{\circ}\text{C}}{\text{W}}\right]. \tag{3}$$

Fig. 6 presents the thermal resistance of the heat sink as a function of Reynolds number for all nozzle combinations tested. The lowest value, $R_{conv} = 0.73$ °C/W, was obtained with the 9 × 1.59 mm array at Re = 15 000 (at an air flow rate of 2237 cm^3/s).

The heat sink thermal resistance R_{conv} is shown in Fig. 7 as a function of volumetric air flow rate for each nozzle plate. When plotted as a function of flow rate (as opposed to Reynolds number), the smaller nozzle diameters provide the lower thermal resistance. The 4 × 3.18 mm array and the 6.35 mm single nozzle nearly overlap in thermal performance in this figure; it appears that the thermal performance is similar for nozzles with the same open area (total nozzle area).

Most of the pressure drop in this cooling technique occurs across the nozzle; this nozzle pressure drop overwhelms any contribution of the presence of the heat sink to pressure drop. In fact, no difference was observed in the measurements of pressure drop with and without the heat sink present for a given nozzle plate for the fin-tip clearance values tested. Fig. 8 shows the pressure drop values for all the experiments of this study as a function of air flow rate. Clearly, the pressure drop at a given flow rate is inversely proportional to the nozzle open area. For example, the 6.35 mm single nozzle has almost the same pressure drop curve as the 4 × 3.18 mm array of the same open area.

For use in problems where pressure drop is the design constraint, R_{conv} is plotted as a function of pressure drop in Fig. 9. It may be noted that a fixed pressure drop across the orifice also corresponds to a fixed mean jet velocity U_{jet}. Both scales are used in Fig. 9. Results are shown for the enhanced and bare surfaces. For instance, at a fixed available pressure drop of 0.14 kPa, the best thermal performance is seen from the figure to be obtained with the single 12.7 mm nozzle.

The product of volume flow rate and corresponding pressure drop represents the pumping power required to deliver the air through the orifices. Fig. 10 shows the pumping power ($\Phi = \Delta P \times \dot{\text{V}}$) required to meet a given thermal resistance requirement for each nozzle configuration. It is evident that significant reductions in heat sink thermal resistance can be achieved for a given pumping power when the number of orifices is increased, or when the orifice diameter is increased for single nozzles. Four nozzle configurations, the single

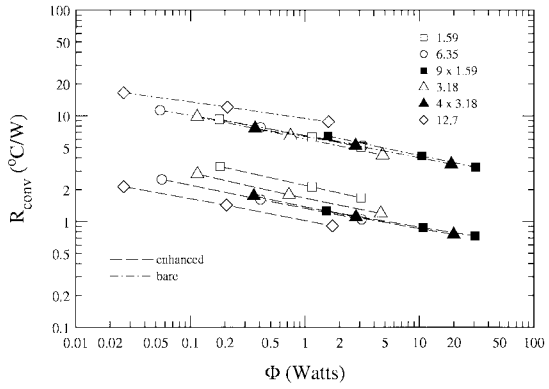

Fig. 10. Thermal resistance of the heat sink and bare surface as a function of pumping power.

nozzles of 3.18 and 6.35 mm diameter and the 4×3.18 mm and 9×1.59 mm nozzle arrays, are seen to perform alike for $0.3 \leq \Phi \leq 4$ W.

IV. Conclusion

Experiments using air jet impingement on a bare and enhanced discrete heated surface were conducted using several single nozzles and multiple-nozzle arrays at different Reynolds numbers. The tests were performed for a fixed nozzle-to-target spacing, (i.e., a fixed fin-tip clearance), since this was not a strong parameter in determining heat transfer rates.

The bare surface experiments showed that for a given Reynolds number, higher heat transfer coefficients were obtained with the smaller diameter nozzles which may be attributed to the associated higher jet velocities. In contrast, the larger single nozzles performed better when the heat sink was present at a given Reynolds number. When compared at a fixed volumetric air flow rate the smaller nozzles provided the lower thermal resistance (higher $\overline{h}$) in both the bare and enhanced surface tests. On the basis of pumping power, the single 12.7 mm diameter nozzle provided the lowest thermal resistance for the enhanced surface tests.

The results obtained from this work provided a basis for understanding confined air jet impingement heat transfer with surface enhancement. Impingement parameters were varied while the enhanced-surface geometry was fixed. It would be desirable in future studies to investigate additional heat sink geometries in order to facilitate a complete optimization analysis. In addition, it would be beneficial to conduct flow visualizations to verify the proposed heat transfer mechanisms.

References

[1] B. W. Webb and C. F. Ma, "Single-phase liquid jet impingement heat transfer," *Adv. Heat Transf.*, vol. 26, pp. 105–217, 1995.
[2] S. V. Garimella and R. A. Rice, "Confined and submerged liquid jet impingement heat transfer," *J. Heat Transf.*, vol. 117, pp. 871–877, 1995.
[3] V. P. Schroeder and S. V. Garimella, "Heat transfer from a discrete heat source in confined air jet impingement," *Heat Transfer*, vol. 5, pp. 451–456, 1998.
[4] ———, "Heat transfer in the confined impingement of multiple air jets," in *Proc. ASME Heat Transfer Div., IMECE*, Anaheim, CA, 1998, vol. HTD-361-1, pp. 183–190.
[5] N. T. Obot and T. A. Trabold, "Impingement heat transfer within arrays of circular jets—Part 1: Effects of minimum, intermediate, and complete crossflow for small and large spacings," *J. Heat Transf.*, vol. 109, pp. 872–879, 1987.
[6] P. F. Sullivan, S. Ramadhyani, and F. P. Incropera, "Use of smooth and roughened spreader plates to enhance impingement cooling of small heat sources with circular liquid jets," *Topics Heat Transf.*, vol. 2, pp. 103–110, 1992.
[7] L. G. Hansen and B. W. Webb, "Air jet impingement heat transfer from modified surfaces," *Int. J. Heat Mass Transf.*, vol. 36, pp. 989–997, 1993.
[8] D. Copeland, "Single-phase and boiling cooling of small pin-fin arrays by multiple slot nozzle suction and impingement," *IEEE Trans. Comp., Packag., Manufact. Technol.*, vol. 18, pp. 510–516, 1995.
[9] ———, "Single-phase and boiling cooling of small pin- fin arrays by multiple nozzle jet impingement," *J. Electron. Packag.*, vol. 118, pp. 21–26, 1996.
[10] K. Minakami, S. Mochizuki, A. Murata, and Y. Yagi, "High performance air cooling for LSIS utilizing a pin-fin heat sink," ASME paper 92-WA/EEP-5, 1992.
[11] C. L. Chapman, S. Lee, and B. L. Schmidt, "Thermal performance of an elliptical pin-fin heat sink," in *Proc. 10th IEEE Semi-Therm*, 1994, pp. 24–25.
[12] Y. C. Lee, W. Zhang, H. Xie, and R. L. Mahajan, "Cooling of a chip package with a 100 W, 1 cm^2 chip," *Adv. Electron. Packag.*, vol. 4, pp. 419–423, 1993.
[13] V. P. Schroeder, "Heat transfer from a discrete heat source in confined air jet impingement with single and multiple orifices," M.S. dissertation, Univ. Wisconsin, Milwaukee, 1997.

Luis A. Brignoni was born in San Juan, Puerto Rico, in 1973. He received the B.S. degree from the University of Puerto Rico, Mayagüez, in 1997 and the M.S. degree from the University of Wisconsin, Milwaukee, in 1999, both in mechanical engineering.

From 1997 to 1999, he worked as a Research Assistant in the Electronics Cooling Laboratory, University of Wisconsin, Milwaukee.

Mr. Brignoni received the Advanced Opportunity Program Fellowship and is a member of the SHPE.

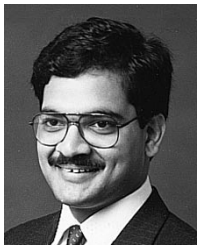

Suresh V. Garimella received the Ph.D. degree from the University of California, Berkeley, and the M.S. degree from The Ohio State University, Columbus.

He is Associate Professor in the School of Mechanical Engineering, Purdue University, West Lafayette, IN. He was previously Cray-Research Associate Professor of Mechanical Engineering at the University of Wisconsin, Milwaukee. He is Director of the Electronics Cooling Laboratory and has recently established the Cooling Technologies Research Consortium to serve industry needs in the area of electronics packaging. His research interests (www.ecn.purdue.edu/ME/Fac_Staff/garimella.whtml) also include crystal growth of electronic materials. He has published eighty technical papers in archival journals and conference proceedings, and has also contributed to, and edited, several books.

Dr. Garimella received the Graduate School/UWM Foundation Research Award in recognition of outstanding research and creative activity in 1995, the UWM Distinguished Teaching Award in recognition of demonstrated dedication to excellence in undergraduate instruction in 1997, and the Society of Automotive Engineers' Ralph R. Teetor Educational Award in 1992. He is on the Editorial Board of *Experimental Thermal and Fluid Science* and a member of the K-16 (Heat Transfer in Electronic Equipment) Committee, Heat Transfer Division, ASME.